Article

p53 reaction to cellular stress maximizes apoptosis in glioblastoma

Cheng-Jung Ho[1], Yu-Hsuan Pao[2¶], Hsin-Wen Chen[2¶], Wei-Hua Zhu[2¶], Ru-Wei Lin[3], Cheng-Wei Chu[4,5], Joon-Khim Loh[4,6], Yi-Ren Hong[7*] and Chihuei Wang[2,8*]

[1]Department of Orthopedics, Kaohsiung Medical University Hospital, Kaohsiung, 807, Taiwan

[2]Department of Biotechnology, Kaohsiung Medical University, Kaohsiung, 807, Taiwan

[3]Graduate Institute of Food Safety Management, National Pingtung University of Science and Technology, Pingtung, 912, Taiwan

[4]Graduate Institute of Medicine, College of Medicine, Kaohsiung Medical University, Kaohsiung, 807, Taiwan

[5]Division of Neurosurgery, Department of Surgery, Kaohsiung Municipal Ta-Tung Hospital, Kaohsiung, 801, Taiwan

[6]Department of Neurosurgery, Kaohsiung Medical University Hospital, Kaohsiung, 807, Taiwan

[7]Department of Biochemistry & Graduate Institute of Medicine, Kaohsiung Medical University, Kaohsiung, 807, Taiwan

[8]Department of Medical Research, Kaohsiung Medical University Hospital, Kaohsiung, 807, Taiwan

[¶]These authors contributed equally to this work.

*Correspondence: chwang@kmu.edu.tw (CW); m835016@cc.kmu.edu.tw (YRH)

Abstract: In prostate cancer, p53 maximizes apoptosis in response to severe DNA damage, not DNA replication stress. Here, we examined the apoptotic response of two glioblastoma cells, p53-wild type U87 and a p53-mutated T98G cell, for the same stresses. We ascertained that p53 intensified apoptosis in response to severe DNA damage, not DNA replication stress in glioblastoma. We further asked if p53-mediated apoptosis can be induced by cellular stress other than severe DNA damage. We analyzed two compounds, bortezomib and vorinostat, respective inhibitors of 26S proteasome and histone deacetylase, to evaluate their capacity to activate p53-mediated apoptosis. The cellular stress incited by bortezomib, not vorinostat, activated p53-mediated apoptosis. Next, we asked if the cellular stress generated by combining the two compounds had a synergistic effect on apoptosis. Our results demonstrated that doxorubicin with bortezomib or CFS-1686, or bortezomib with vorinostat have a significant synergistic effect on apoptosis only in p53-wild type cell. Under high stress, p53 translocates from cytosol into the nucleus to cause apoptosis possibly. Together, p53 maximizes apoptosis for cellular stress caused by severe DNA damage, disruption of protein turnover, and for the stress induced by drug combination including doxorubicin with bortezomib or CFS-1686, and bortezomib with vorinostat.

Keywords: glioblastoma; p53; apoptosis; doxorubicin; bortezomib; vorinostat.

1. Introduction

p53 is regarded as the most important cancer-suppressing gene *in vivo*. *p53* also has an essential role in cancer-therapeutic apoptosis. When cancer cells are treated by agents that disrupt cellular activities, p53 is activated by shutting down its negative regulator, MDM2, to turn on the numerous target genes [1, 2]. Several of these are involved in cell cycle arrest, DNA repair and apoptosis in response to treatment [3, 4].

Preprints (www.preprints.org) | NOT PEER-REVIEWED | Posted: 30 January 2019 doi:10.20944/preprints201901.0315.v1

The target genes of p53 participating in cell cycle arrest and DNA repair include *p21*, *GADD45A*, *DDB2*, *FANCC* and *XPC,* which function to rescue cells from damage [5, 6]. Another group of p53-upregulated genes including *PUMA*, *NOXA*, *BAX* and *APAF* do the opposite way and propel cell death through apoptosis [5, 6]. We may ask how cell fate, either survival or death, can be determined by the same p53 molecule after treatment with genotoxic agents. The theory of promoter selectivity proposes that p53 interacts differentially with its response elements through post-translational modifications and interactions with cofactors to activate cell survival or apoptosis genes [7]. However, several microarray studies analyzing genotoxic expression profiles after p53 overexpression revealed that both cell cycle arrest and apoptosis genes are transcribed by the same conditions [8-11]. One study claimed that the level of p53 is a threshold mediating the cell fate decision between growth arrest and apoptosis [12].

In addition, two studies have demonstrated that p53 is not a transcriptional activator of Puma in prostate cancer [13, 14]. Instead of Puma, another BH3-only protein, Bim, counteracts Bcl-xl to initiate apoptosis in a p53-independent manner for doxorubicin-treated prostate cancer [14]. Our recent study further found that the role of p53 is to intensify apoptosis after doxorubicin-induced DNA damage stress, not to activate Puma to initiate apoptosis, and that DNA replication stress-induced apoptosis is p53-independent in prostate cancer [15].

To see if the p53-mediated apoptosis found in prostate cancer also occurs in other cancer types, we extended our studies to glioblastoma. Two widely studied cell lines, U87 and T98G, were generated over 50 years ago from glioblastoma patients [16, 17]. U87 carries wild type *p53* [18] and T98G has a mutation at codon 273 (ATG to ATA) of *p53* that blocks transcriptional activity in reporter gene assay [19]. Using this pair of glioblastoma cell lines, we asked if cellular stress caused by a given single agent or combination of two agents can induce apoptosis through either a p53-dependent or p53-independent pathway. Our results revealed that doxorubicin and bortezomib induce p53-mediated apoptosis dose-responsively, while CFS-1686 and vorinostat trigger apoptosis in a p53- and dose-independent manner. Three combinations, doxorubicin plus CFS-1686, doxorubicin plus bortezomib and bortezomib plus vorinostat, all produce synergistic apoptosis in a p53-dependent manner. The determining factor for p53-mediated apoptosis from either a single agent or a combination of two agents is the extent or type of cellular stress, not the level of p53.

2. Results

2.1. The effects of doxorubicin can be divided into two phases by the dual role of p53 in U87 cells, while CFS-1686-induced apoptosis is p53-independent

The role of p53 is to maximize apoptosis in response to severe DNA damage, not to activate BH3-only protein to initiate apoptosis, in prostate cancer [15]. We investigated various responses of U87 cells including the level of p53, the expression of BH3-only proteins, cell cycle arrest, DNA damage and apoptosis in the presence of doxorubicin from low to high concentration. The results revealed that the level of p53 kept increasing as doxorubicin concentrations increased, up to maximum at 0.5 μM, and then declined from 0.5 μM to 2 μM (Fig 1A). Interestingly, the expression of p21, the sign of cell cycle arrest, appeared at 0.125 μM and dropped to basal levels at 0.5 μM (Figure 1A). In contrast, the activation of caspase 3, the sign of apoptosis, showed up at 0.5 μM and reached maximum at 1 μM (Figure 1A). Cell cycle arrest and apoptosis corresponded to low and high DNA damage,

Preprints (www.preprints.org) | NOT PEER-REVIEWED | Posted: 30 January 2019 doi:10.20944/preprints201901.0315.v1

respectively, as evaluated by the level of γH2AX (Figure 1A). The functions of p53 in the above two events can be easily distinguished in U87 cells. In addition, the expression of Puma was not affected by p53 (Figure 1A), suggesting that the canonical pathway of p53-mediated apoptosis does not occur in this cell.

Unlike U87 cells, doxorubicin treatment in T98G cells did not activate caspase 3, even at concentrations up to 7-fold higher than in the positive control U87 cell (Figure 1B). We then asked if doxorubicin has any effect on T98G cells. The result revealed that doxorubicin caused DNA damage though it cannot activate p21 expression via its mutated p53, compared to U87 cells treated by 0.25 μM of doxorubicin showing high expression of p21 (Figure 1C). Thus, we concluded that the mutated form of p53 in T98G is not a functional form of p53 and cannot effectively induce apoptosis in T98G (Figure 1B).

We further tested the effect of CFS-1686-induced DNA replication stress on apoptosis in T98G and U87 cells. This compound has been verified as the catalytic inhibitor of topoisomerase 1 [20] and it can induce apoptosis in prostate cancer independently of p53 [15]. Here, CFS-1686 could induce apoptosis in both U87 and T98G cells with about equal sensitivity, suggesting that apoptosis in response to DNA replication stress is p53-independent in glioblastoma (Figure 1D). However, this apoptosis-initiating compound showed no capacity to maximize apoptosis by increasing its concentration higher than 1 μM (Figure 1D).

Our results clearly indicated that apoptosis can be initiated either with or without p53 and the role of p53 is to magnify the apoptotic death signal dependent on the type and magnitude of cell stress in glioblastoma.

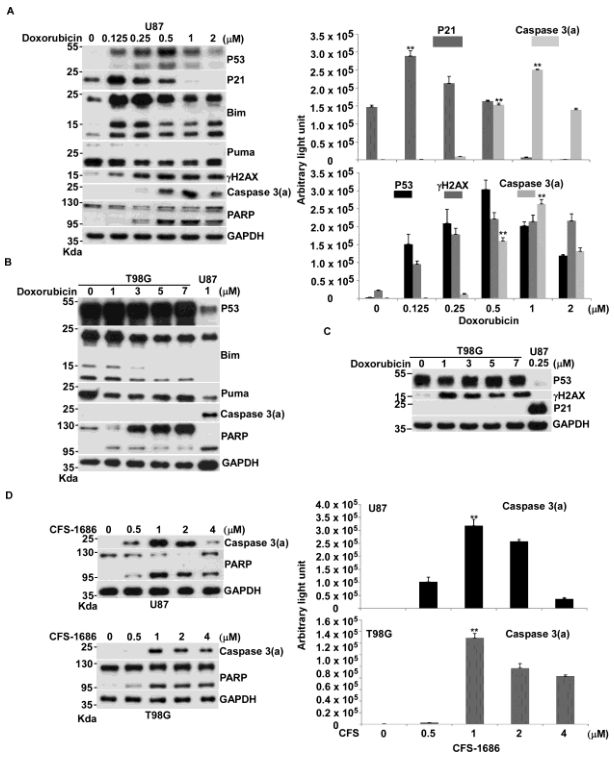

Figure 1. Doxorubicin-induced apoptosis was p53-dependent, while CFS-1686-induced apoptosis was p53-independent in glioblastoma. A) The highest level of apoptosis corresponds with the extent of DNA damage, not to the highest expression of p53 in U87 cells. U87 cells were incubated with various concentrations of doxorubicin

Preprints (www.preprints.org) | NOT PEER-REVIEWED | Posted: 30 January 2019 doi:10.20944/preprints201901.0315.v1

for 24 h and harvested for western blotting. The immunoblot images of p21, the activation form of caspase 3, caspase 3(a), p53, and γH2AX, normalized to GAPDH, were quantitated as shown. B) Doxorubicin could not induce apoptosis effectively in T98G cells. T98G cells were incubated with various concentrations of doxorubicin for 24 h and harvested for western blotting. U87 cell treated with 1 μM of doxorubicin served as a positive control. C) Doxorubicin caused DNA damage in T98G cells. T98G cells were incubated with various concentrations of doxorubicin as indicated for 24 h and harvested for western blotting. U87 cells treated with 1 μM of doxorubicin served as a control to show the expression of p21. D) CFS-1686, which causes DNA replication stress, induced apoptosis in both T98G and U87 cells. T98G and U87 cells were incubated with various concentrations of CFS-1686 for 24 h and harvested for western blotting. Immunoblot images of the activation form of caspase 3, caspase 3(a), were quantitated as shown.

2.2. Bortezomib and vorinostat induced apoptosis in a dose-dependent and -independent manner, respectively.

Since p53-mediated apoptosis has selectivity for stress types, we further explored whether cellular stresses other than DNA damage can be sensed by p53 to enhance apoptotic response. We analyzed two chemotherapeutic agents, bortezomib and vorinostat, respective inhibitors of 26S proteasome [21] and histone deacetylase [22] , for their potential to activate p53-mediated apoptosis in U87 cells and T98G cells.

Bortezomib stabilized p53 at a constant level from 0.01 μM to 0.15 μM and induced apoptosis in dose-dependent fashion in U87 cells (Figure 2A). Interestingly, bortezomib could also induce apoptosis in T98G cells at high concentrations, starting at 0.05 μM, but the activation form of caspase 3 remained almost the same from 0.1 μM to 1 μM (Figure 2A). We speculated that the differential response of U87 and T98G cells to bortezomib is due to the presence and absence of functional p53, respectively. In U87 cells, p53 reacted to the increasing cellular stress induced by the increasing concentration of bortezomib by dose-responsive apoptosis. However, though bortezomib-induced cellular stress could initiate apoptosis, it had no capacity to amplify apoptosis in T98G cells without p53. Thus bortezomib-induced apoptosis might be p53-dependent.

In contrast, vorinostat could induce apoptosis without increases in p53 and even a reduced basal level of p53 in U87 cells (Figure 2B). The apoptotic signal, the activation form of caspase 3, remained almost unchanged with increasing concentrations of vorinostat from 4 μM to 10 μM (Figure 2B). In T98G cells without functional p53 vorinostat could not trigger apoptosis effectively and showed no dose-responsive pattern of PARP cleavage (Figure 2B). These results suggested that vorinostat-induced cellular stress could only initiate apoptosis, and this stress could not be sensed by p53. Vorinostat-induced apoptosis might be regarded as p53-independent.

We then used the nucleus/cytosol fraction to examine the distribution of p53 between the nucleus and cytosol in apoptosis or non-apoptosis conditions. An increase in the p53 ratio of nucleus to cytosol along with increasing apoptosis was seen in doxorubicin-and bortezomib-treated U87 cells (Figure 2C). For doxorubicin-treated cells, the respective p53 ratios of nucleus to cytosol at 0.125 μM and 1 μM were about 1.8 and 4.7, corresponding to p53 cell cycle arrest and apoptosis functions (Figure 1A and Figure 2C). This suggested that apoptosis activation might require more nuclear p53 than cell cycle arrest activation. The lowest p53 ratios of nucleus to cytosol appeared in bortezomib-treated cells at 0.01 μM, about 0.2, with no apoptosis at this ratio (Figure 2A and C). By increasing the

Preprints (www.preprints.org) | NOT PEER-REVIEWED | Posted: 30 January 2019 doi:10.20944/preprints201901.0315.v1

concentration of bortezomib up to 0.150 μM, the p53 ratio of nucleus to cytosol increased about 4-fold to 0.85, resulting in significant apoptosis (Figure 2A and C). This was a comparatively low p53 ratio of nucleus to cytosol, compared to the ratio from doxorubicin-treated cells. It seems likely that different types of cellular stress require different amounts of nuclear p53 to induce apoptosis.

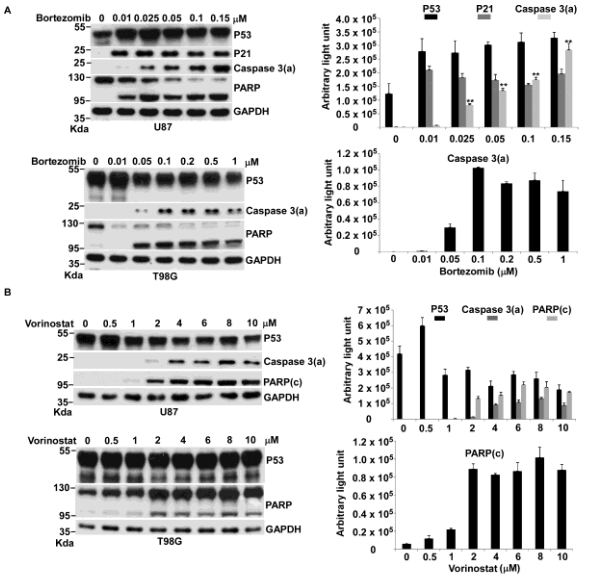

Figure 2. Bortezomib or vorinostat induced apoptosis in dose-independent manner Bortezomib caused the dependent or and induced apoptosis respectively. A) manner in U87 cells, stabilization of p53 in a dose-dependent while it induced apoptosis in dose-independent manner in T98G cells. Immunoblot images of p53, the activation form of caspase 3, caspase 3(a), and p21 normalized to GAPDH, were quantitated as shown. B) Vorinostat reduced the basal level of p53 and induced apoptosis dose-independently in U87 cells, while it could not effectively induce apoptosis in T98G cells. The immunoblot images of p53, the activation form of caspase 3, caspase 3(a), and the cleaved PARP normalized to GAPDH were quantitated as shown. Experimental conditions of A) and B) were similar to those in fig 1A. C) Doxorubicin or bortezomib caused the translocation of p53 from cytosol to nucleus in U87 cells. U87 cells were incubated with 0.125 and 1 μM of doxorubicin or with 0.01 and 0.15 μM of bortezomib for 24 h and harvested for nucleus and cytosol fractionation. Fractionated nucleus and cytosol protein were further analyzed by western blotting. The p53 ratio of nucleus to cytosol was quantitated as shown. N: nucleus; C: cytosol; p53(N): p53 in nucleus; p53(C): p53 in cytosol.

2.3. Apoptosis induced by bortezomib was p53-dependent.

From the above result, we speculated that bortezomib-induced apoptosis might be p53-dependent. We still could not draw the conclusion that p53 plays an essential role in bortezomib-induced apoptosis, without direct evidence. We used overexpression of p53 in LNCaP cells, a prostate can cell line containing a wild type p53, to see if p53 was really involved in bortezomib-induced apoptosis. We previously used the same approach to address whether p53 is responsible for doxorubicin-induced apoptosis after heavy DNA damage condition[15]. Interestingly, our results

Preprints (www.preprints.org) | NOT PEER-REVIEWED | Posted: 30 January 2019 doi:10.20944/preprints201901.0315.v1

clearly demonstrated that p53 overexpression enhanced apoptosis in response to bortezomib (Figure 3A). We concluded that p53 does react to the cellular stress caused by bortezomib, resulting in the maximization of apoptosis.

However, p53 was unable to redeem bortezomib-induced apoptosis in PC3 cells, which is a p53-null prostate cancer cell line (Figure 3B). p53 overexpression cannot enhance doxorubicin-induced apoptosis in PC3 cells [15]. Thus, it appears that p53-mediated apoptosis in response to various agent-induced cell stresses might go through a common, but complicated mechanism requiring the involvement of other factors. Those factors might not be present in PC3 cells.

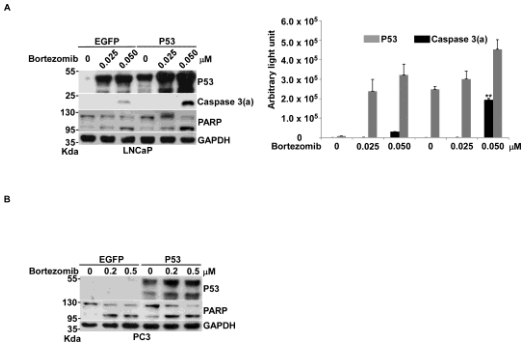

Figure 3. Bortezomib-induced apoptosis was p53-dependent. A) Overexpression of p53 increased bortezomib-induced apoptosis in LNCaP cells. The plasmids for the expression of EGFP and p53 were transfected into LNCaP cells by electroporation. The transfected cells were cultured for 2 days, then incubated with 0.025 and 0.050 μM of bortezomib for 36 h and harvested for western blotting. The immunoblot images of p53 and the activation form of caspase 3, caspase 3(a) normalized to GAPDH, were quantitated as shown. B) The overexpression of p53 did not increase bortezomib-induced apoptosis in PC3 cells. The respective plasmids for the expression of EGFP and p53 were transfected into PC3 cells by FuGENE 6. The transfected cells were cultured for 24 h, then incubated with 0.2 and 0.5 μM bortezomib for 36 h and harvested for western blotting.

2.4. The combination of doxorubicin with bortezomib had a significant synergistic effect on apoptosis, while the combination of doxorubicin with vorinostat slightly lowered apoptosis compared to doxorubicin alone.

Bortezomib and vorinostat are new-generation chemotherapy agents that alter cellular functions other than targeting DNA or microtubules and show some convincing responses in certain cancer types in the clinic. Interestingly, the cellular stresses generated by bortezomib and vorinostat have different effects on p53 and apoptosis in glioblastoma. We explored the effect of combining doxorubicin with p53-dependent bortezomib or p53-independent vorinostat on apoptosis in U87 or T98G cells.

The combination of two p53-dependent agents, doxorubicin plus bortezomib, showed a strong synergistic dose-dependent effect on apoptosis in U87 cells, but not in T98G cells (Figure 4A). Doxorubicin and bortezomib induce apoptosis through p53. T98G cells contain non-functional p53 and did not show increased apoptosis with this combination (Figure 4A). Thus, we speculated that this synergistic apoptosis effect might be p53-dependent. Interestingly, the level of p53 did not increase with this combination in U87 cells (Figure 4A), which indicated that the level of p53 did not determine this synergistic effect. The cellular stress generated by the combination of doxorubicin with bortezomib was much higher than with doxorubicin or bortezomib alone. Thus, we thought that the extent of cellular stress might be a factor to determine the magnitude of apoptosis.

Preprints (www.preprints.org) | NOT PEER-REVIEWED | Posted: 30 January 2019 doi:10.20944/preprints201901.0315.v1

The p53 ratio of nucleus to cytosol from the combination of doxorubicin to bortezomib was about 1.3 (Figure 4B). This value was a little higher than the ratio from bortezomib alone (about 1) and lower than the ratio from doxorubicin (about 1.6, Figure 4B). This result suggested that translocation of p53 into the nucleus seemed essential for apoptosis, while the synergistic effects were determined by compounded cellular stresses caused by the doxorubicin/bortezomib combination (Figure 4A).

Conversely, the apoptotic response induced by combining doxorubicin with vorinostat was lower than that induced by doxorubicin alone (Figure 4C). This was an interesting example of a negative effect from a two-drug combination. Further studies are required to explain this negative effect.

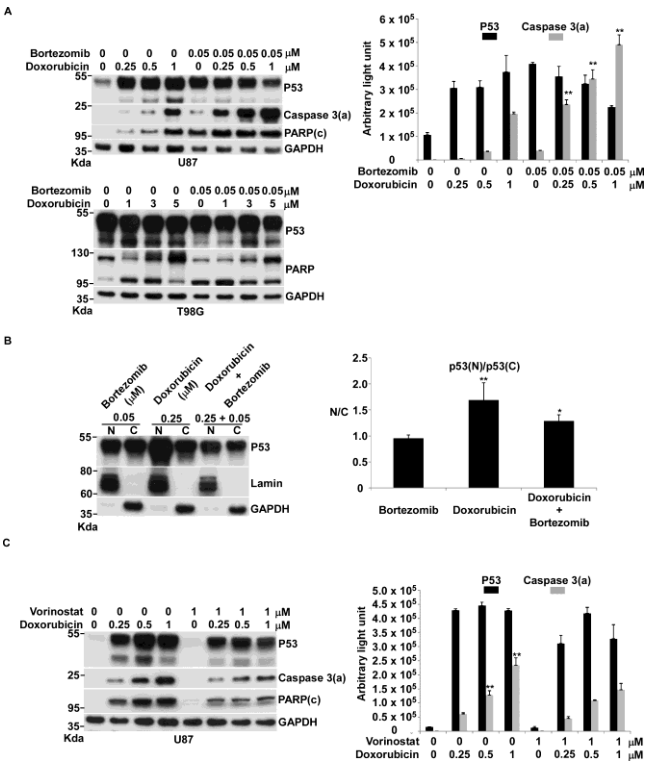

Fig 4. The combination of doxorubicin with bortezomib, but not vorinostat, induced apoptosis synergistically in U87 cells. A) The doxorubicin/bortezomib combination had a synergistic effect on apoptosis in U87 cells, but not in T98G cells. U87 or T98G cells were incubated with various concentrations of doxorubicin alone or with 0.05 μM of bortezomib for 24 h and harvested for western blotting. The immunoblot images of p53 and the activation form of caspase 3, caspase 3(a) normalized to GAPDH, were quantitated as shown. B) The nucleus to cytosol ratio of p53 was higher with doxorubicin plus bortezomib than bortezomib alone. Experimental conditions were similar to fig 2C. The nucleus to cytosol ratio of p53 was quantitated as shown. C) Vorinostat had a negative effect on doxorubicin-induced apoptosis in U87 cells. Experimental conditions were similar to those in A.

2.5. The combination of doxorubicin plus CFS-1686 or bortezomib plus vorinostat had significant synergistic effects on apoptosis.

The above experiment showed that combining a p53-dependent compound with a p53-independent compound lowered the apoptotic response (Figure 4B). We asked if other p53-independent agents can interfere with p53-dependent compound-induced apoptosis. We explored two combinations of a p53-dependent compound with a p53-independent compound including doxorubicin plus CFS-1686 and bortezomib plus vorinostat.

Preprints (www.preprints.org) | NOT PEER-REVIEWED | Posted: 30 January 2019 doi:10.20944/preprints201901.0315.v1

To our surprise, both combinations demonstrated a synergistic dose-responsive effect on apoptosis in U87 cells, but not in T98G cells (Figure 5A and B). Since both doxorubicin- and bortezomib-induced apoptosis are p53-dependent, we thought p53 might play an essential role for these two combination-induced apoptotic responses. However, the level of p53 did not increase from these combinations, suggesting that the synergistic effects on apoptosis might be determined by cellular stress, as seen with the combination of doxorubicin and bortezomib. We propose that the cellular stresses caused by these drug combinations are not merely additive and might induce a complex combination of stresses.

The p53 ratio of nucleus to cytosol from the combination of CFS-1686 with doxorubicin was about 3, almost equal to that of doxorubicin alone (Figure 5C). Most p53 will have translocated into the nucleus at this value (Figure 5C). The p53 inside the nucleus might be available for enhancing apoptosis under the huge cellular stress caused by the combination of CFS-1686 with doxorubicin with the results shown in figure 5A.

Unlike doxorubicin, which has a big capacity to drive p53 from cytosol to nucleus, translocation of p53 to the nucleus was relatively limited in bortezomib-treated U87 cells. Even at concentrations up to 0.150 μM that trigger efficient apoptosis, the p53 ratio of nucleus to cytosol in bortezomib-treated cells was about 0.85 (Figure 2C). Significantly, the p53 ratio of nucleus to cytosol for the combination of bortezomib with vorinostat was 1.6, 3-fold and 9-fold higher than that of bortezomib and vorinostat, respectively (Figure 5D). We speculate that the nuclear translocation of p53 driven by this combination generates the synergistic effect on apoptosis shown in figure 5B.

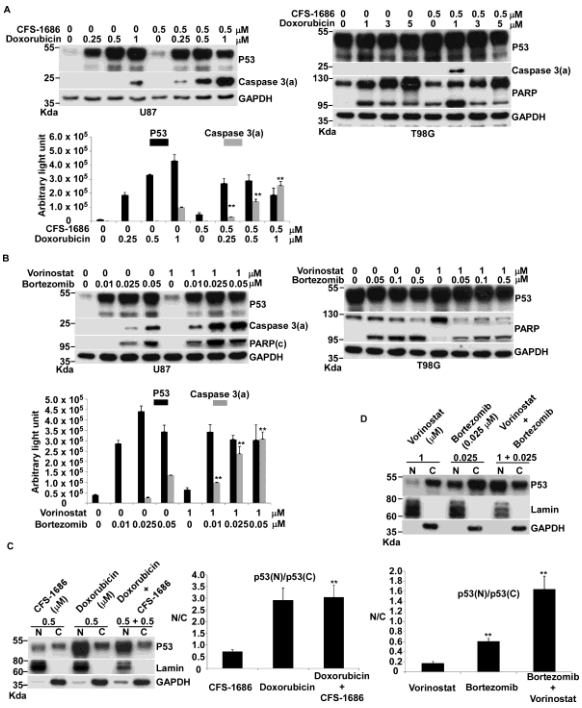

Figure 5. The combination of doxorubicin with CFS-1686 or the combination of bortezomib with vorinostat induced synergistic apoptosis in U87 cells, but not in T98G cells. A) Doxorubicin plus CFS-1686 induced a synergistic apoptotic response in U87, but not T98G cells. The immunoblot images of p53 and the activation form of caspase 3, caspase 3(a) normalized to GAPDH, were quantitated as shown. B) Bortezomib plus vorinostat induced synergistic apoptosis in U87, but not in T98 cells. The immunoblot images of p53 and the activation form of caspase 3, caspase 3(a)

Preprints (www.preprints.org) | NOT PEER-REVIEWED | Posted: 30 January 2019 doi:10.20944/preprints201901.0315.v1

normalized to GAPDH, were quantitated as shown. Experimental conditions of A) and B) were similar to fig 4A. C) The nucleus to cytosol ratio of p53 was higher for doxorubicin plus CFS-1686 than CFS-1686 alone. The nucleus to cytosol ratio of p53 was quantitated as shown. D) The nucleus to cytosol ratio of p53 was higher in bortezomib plus vorinostat than either bortezomib or vorinostat alone. The nucleus to cytosol ratio of p53 was quantitated as shown. Experimental conditions of C) and D) were similar to fig 2C.

3. Discussion

Our results revealed that doxorubicin, bortezomib, doxorubicin plus CFS-1686, doxorubicin plus bortezomib or bortezomib plus vorinostat induced cellular stresses that could be sensed by p53. In contrast, CFS-1686 or vorinostat-induced cellular stress could not be sensed by p53. Cellular stresses that caused a reaction by p53 produced a magnitude of apoptosis proportional with the extent of cellular stress, eventually up to maximum when cellular stress reached the utmost (Fig 6). However, cellular stress that could not be sensed by p53 only initiated a level of apoptosis that remained constant and could not be amplified (Figure 6).

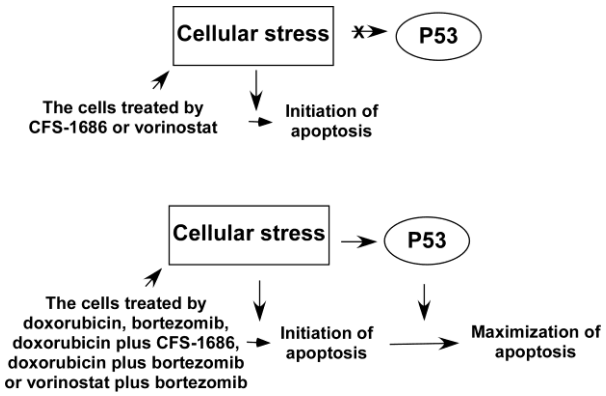

Figure 6. Two factors, cellular stress and p53 status, determine maximization of apoptosis in glioblastoma cells.

Our study raises a very interesting issue about the stress selectivity of p53. Among the four compounds we studied, doxorubicin and bortezomib displayed p53-dependent effects, while CFS-1686 and vorinostat showed p53-independent effects. Based on the types of cellular stress, doxorubicin and bortezomib caused DNA double-strand breaks and shutdown of protein turnover, which were more threatening to cell survival than halt in DNA replication or the unwinding of chromatin structures caused by CFS-1686 or vorinostat, respectively. Thus, we concluded that the stress selectivity of p53 is based on the severity of the cellular stress. This speculation is fully supported by the combination treatments that showed synergistic outcomes of p53-mediated apoptosis, because these combination treatments seemed to generate more cellular stress than either compound used alone.

One study has proposed that the level of p53 is a threshold determining the cell fate of either cell cycle arrest or apoptosis, and that lowering the apoptotic threshold can potentially increase p53-mediated apoptosis[12]. Our results demonstrated that apoptosis began at 0.5 μM and reached maximum at 1 μM of doxorubicin in U87 cells (Figure 1A). However, the status of apoptosis corresponded to the level of γH2AX, not p53 (Figure 1A). Moreover, the magnitude of apoptosis matched the concentration of bortezomib, not the level of p53, in bortezomib-treated U87 cells (Fig

 doi:10.20944/preprints201901.0315.v1

2A). In the three combination treatments we explored, doxorubicin plus bortezomib, doxorubicin plus CFS-1686 and bortezomib plus vorinostat, the synergistic effect of apoptosis was not correlated with the level of p53, but did parallel the extent of cellular stress (Figure 4A and Figure 5A and B). Thus, we speculated that the threshold of p53-mediated action is the extent of cellular stress, not the level of p53.

The type and extent of cellular stress therefore controls p53-mediated apoptosis in glioblastoma. Our results demonstrated that the translocation of p53 from cytosol to nucleus seems to be an essential step in p53's initiation of apoptosis. According to the canonical p53-mediated apoptotic pathway, once in the nucleus p53 transcriptionally activates Puma or Noxa to trigger apoptosis. However, the expression of Puma was not affected by p53 (figure 1A), and two p53-independent agents, CFS-1686 and vorinostat, could also initiate apoptosis (Figure 1D and Figure 2B). These results excluded the canonical p53-mediated apoptotic pathway as the cause of p53-initiated apoptosis in glioblastoma. Other target genes of p53 might be involved in this pathway.

4. Materials and Methods

4.1. Compounds and plasmids

Doxorubicin (Merck Millipore), bortezomib (Selleck), vorinostat (Selleck) and FuGENE 6 (Promega) were purchased as indicated. CFS-1686 is an in-house compound [20]. The two plasmids including pCMV-p53 and pIRES2-EGFP (Clontech), which were used for overexpression of p53 and vehicle control for transfection, respectively, were purchased as indicated.

4.2. Cell culture and compound treatment

The U87 and T98G glioblastoma cell lines and LNCaP and PC3 prostate carcinoma cell lines were obtained from the Bioresource Collection and Research Center (BCRC) in Taiwan. Culture conditions for all four cells were 37°C under 5% CO_2 in their respective medium with 10% fetal bovine serum. RPMI 1640 (Invitrogen) medium was used for the two prostate cancer lines. The media for U87 and T98G were α-MEM (Invitrogen) and DMEM (Invitrogen) respectively. About 5×10^5 cells of LNCaP or PC3 and 1 x 10^5 cells of U87 or T98G were plated on petri dish (10 cm). When cell growth was reached 70-80% confluence, fresh medium was substituted and the cells were incubated with various concentrations of doxorubicin, CFS-1686, bortezomib, vorinostat or various combinations for 24 h. After treatment the cells were harvested, washed with PBS and spun down.

4.3. Cell transfection

For transfection of LNCaP cells**,** 5 plates (10 cm) of LNCaP cells at 70% confluence were collected and re-suspended in 0.8 ml of serum-free RPMI 1640 medium. Then, 0.8 ml of cells were aliquoted into two Gene Pulser Cuvetts (Bio-Rad) each containing 0.4 ml of cells. Then 5 μg of pCMV-p53 or pIRES2-EGFP were added to each cuvette. The cells in the cuvette were electroporated by Bio-Rad Gene Pulser at 230 volts and 960 μFaraday. Following transfection, the cells were collected, washed and plated into 3 plates (10 cm) and incubated with RPMI 1640 media containing 10% FBS for 2 days. Then the cultured medium was replaced by fresh medium with various concentrations of bortezomib for 36 h and the cells were harvested for immunoblotting. For PC3 cells, we used FuGENE 6 to

Preprints (www.preprints.org) | NOT PEER-REVIEWED | Posted: 30 January 2019 doi:10.20944/preprints201901.0315.v1

perform transfection. We mixed 26 μl of FuGENE 6 transfection reagent with 340 μl of RPMI 1640 serum-free medium, and incubated for 5 min. About 6 μg of DNA were added to the FuGENE 6/medium mixture and incubated for 15 min. Then the DNA solution was added to the cultured PC3 cells (10 cm dish, about 70% confluence) dropwise. The transfected PC3 cells were incubated for 24 h. Then, the cultured medium was replaced by fresh medium with various concentrations of bortezomib for 36 h and the cells were harvested for immunoblotting.

4.4. Cytosol and nuclear fractionation

Three plates of U87 cells treated by the same compound or compound combination were harvested and then washed in hypotonic buffer (10 mM Hepes pH7.9, 1.5 mM $MgCl_2$, 10 mM KCl, 0.5 mM DTT) with protease and phosphatase inhibitors. The washed cell pellets were resuspended in hypotonic buffer for 10 min to swell cells. The swollen cells were homogenized by 5 up-and-down pushes through the syringe with 26 1/2 needle. The nuclei were spun down by centrifuging for 15 min at 4000 rpm. After spinning down, the cytosol supernatant and the collected nuclei were lysed in RIPA buffer (25 mM Tris-HCl pH7.6, 150 mM NaCl, 1% NP40 1 mM DTT, 0.1% NP-40, 1% sodium deoxycholate, 0.1% SDS) containing protease and phosphatase inhibitors. Both cytosol and the nuclei lysates were analyzed by immunoblotting.

4.5. Immunoblotting

The harvested cells were lysed in RIPA buffer containing protease and phosphatase inhibitors. The protein concentrations from the cell lysate, separated cytosol and nuclear lysate were determined by a BCA Protein Assay Kit (Pierce). About 60 μg of protein per well was subjected to SDS-PAGE. After electrophoresis, the proteins were transferred to a nitrocellulose membrane. The transferred membranes were blocked in 5% (w/v) nonfat dry milk or 5% (w/v) BSA in TBS (0.5 M NaCl, 20 mM Tris-HCl, pH 7.4) with 0.1% (v/v) Tween 20 and probed for the first antibody, followed by incubation with a secondary antibody conjugated with horseradish peroxidase (anti-rabbit, Cell Signaling; anti-mouse, Jackson ImmunoResearch) with visualization by ECL (Merck Millipore) with photographic film development. The first antibodies used in this study were anti-GAPDH (Cell Signaling, #5174), anti-Bim (Cell Signaling, #2933), anti-caspase 3(a) (Cell Signaling, #9661), anti-PARP (Cell Signaling, #9542), anti-γH2AX (Santa Cruz Biotechnology, Sc-517348), anti-p21 (Abcam, ab109199), anti-Puma (Cell Signaling, #4976), anti-lamin (Cell signaling, #4777) and anti-p53 (Santa Cruz Biotechnology, Sc-126). Immunoblot images were quantitated by Image Studio Lite (LI-COR Biosciences).

4.6. Statistical analysis

A paired t-test was used to show the statistical significance of the results using JMP13. *$P < 0.05$ or **$P < 0.01$ was considered significant.

5. Conclusions

In conclusion, we found that the cellular stress caused by doxorubicin, bortezomib, or three combinations including doxorubicin plus bortezomib, doxorubicin plus CFS-1686 and bortezomib plus vorinostat can trigger p53-mediated apoptosis, but not CFS-1686 or vorinostat. The extent of cellular stress, not the level of p53, appears to be the threshold determining p53-mediated apoptosis.

Author Contributions: "conceptualization, CW; CJH and YRH.; methodology, YHP; HWC; WHZ and RWL.; software, YHP; HWC; WHZ and RWL.; validation, YHP; HWC; WHZ and RWL.; formal analysis, YHP; HWC; WHZ and RWL.; investigation, CW and CJH.; resources, CW; JKL; CWC and YRH.; data curation, YHP; HWC; WHZ and RWL.; writing—original draft preparation, CJH.; writing—review and editing, CW and YRH.; supervision, CW.; funding acquisition, CW; CJH and JKL.

Funding: This research was funded by Kaohsiung Medical University, KMU-M107012(CW), by Kaohsiung Municipal Ta-Tung Hospital, kmtth-106-017 (CJH) and by Kaohsiung Municipal Siaogang Hospital, kmhk-104-007 (JKL).

Acknowledgments: The authors thank Gary Mawyer, M.F.A., for manuscript editing.

Conflicts of Interest: The authors declare no conflict of interest. The funders had no role in the design of the study; in the collection, analyses, or interpretation of data; in the writing of the manuscript, or in the decision to publish the results.

References

1. Vazquez A, Bond EE, Levine AJ, Bond GL. The genetics of the p53 pathway, apoptosis and cancer therapy. Nature reviews Drug discovery. 2008;7(12):979-87.
2. Lavin MF, Gueven N. The complexity of p53 stabilization and activation. Cell death and differentiation. 2006;13(6):941-50.
3. Kastenhuber ER, Lowe SW. Putting p53 in Context. Cell. 2017;170(6):1062-78.
4. Brady CA, Attardi LD. p53 at a glance. Journal of cell science. 2010;123(Pt 15):2527-32.
5. Fischer M. Census and evaluation of p53 target genes. Oncogene. 2017;36(28):3943-56.
6. Vousden KH, Lu X. Live or let die: the cell's response to p53. Nature reviews. 2002;2(8):594-604.
7. Murray-Zmijewski F, Slee EA, Lu X. A complex barcode underlies the heterogeneous response of p53 to stress. Nature reviews Molecular cell biology. 2008;9(9):702-12.
8. Kaeser MD, Iggo RD. Chromatin immunoprecipitation analysis fails to support the latency model for regulation of p53 DNA binding activity in vivo. Proceedings of the National Academy of Sciences of the United States of America. 2002;99(1):95-100.
9. Szak ST, Mays D, Pietenpol JA. Kinetics of p53 binding to promoter sites in vivo. Molecular and cellular biology. 2001;21(10):3375-86.
10. Robinson M, Jiang P, Cui J, Li J, Wang Y, Swaroop M, et al. Global genechip profiling to identify genes responsive to p53-induced growth arrest and apoptosis in human lung carcinoma cells. Cancer biology & therapy. 2003;2(4):406-15.
11. Zhao R, Gish K, Murphy M, Yin Y, Notterman D, Hoffman WH, et al. Analysis of p53-regulated gene expression patterns using oligonucleotide arrays. Genes & development. 2000;14(8):981-93.
12. Kracikova M, Akiri G, George A, Sachidanandam R, Aaronson SA. A threshold mechanism mediates p53 cell fate decision between growth arrest and apoptosis. Cell death and differentiation. 2013;20(4):576-88.
13. Dey P, Strom A, Gustafsson JA. Estrogen receptor beta upregulates FOXO3a and causes induction of apoptosis through PUMA in prostate cancer. Oncogene. 2014;33(33):4213-25.
14. Yang MC, Lin RW, Huang SB, Huang SY, Chen WJ, Wang S, et al. Bim directly antagonizes Bcl-xl in doxorubicin-induced prostate cancer cell apoptosis independently of p53. Cell cycle (Georgetown, Tex. 2016;15(3):394-402.
15. Lin RW, Ho CJ, Chen HW, Pao YH, Chen LE, Yang MC, et al. P53 enhances apoptosis induced by doxorubicin only under conditions of severe DNA damage. Cell cycle (Georgetown, Tex. 2018;17(17):2175-86.

 doi:10.20944/preprints201901.0315.v1

16. Westermark B, Ponten J, Hugosson R. Determinants for the establishment of permanent tissue culture lines from human gliomas. Acta Pathol Microbiol Scand A. 1973;81(6):791-805.
17. Stein GH. T98G: an anchorage-independent human tumor cell line that exhibits stationary phase G1 arrest in vitro. Journal of cellular physiology. 1979;99(1):43-54.
18. Hirose Y, Berger MS, Pieper RO. p53 effects both the duration of G2/M arrest and the fate of temozolomide-treated human glioblastoma cells. Cancer research. 2001;61(5):1957-63.
19. Van Meir EG, Kikuchi T, Tada M, Li H, Diserens AC, Wojcik BE, et al. Analysis of the p53 gene and its expression in human glioblastoma cells. Cancer research. 1994;54(3):649-52.
20. Lin RW, Yang CN, Ku S, Ho CJ, Huang SB, Yang MC, et al. CFS-1686 causes cell cycle arrest at intra-S phase by interference of interaction of topoisomerase 1 with DNA. PloS one. 2014;9(12):e113832.
21. Adams J, Kauffman M. Development of the proteasome inhibitor Velcade (Bortezomib). Cancer investigation. 2004;22(2):304-11.
22. Grant S, Easley C, Kirkpatrick P. Vorinostat. Nature reviews Drug discovery. 2007;6(1):21-2.